12-2019

Raman investigations on gamma irradiated iPP-VGCNF nanocomposites: The polymer's tale

Dorina M. Chipara
The University of Texas Rio Grande Valley, dorina.chipara@utrgv.edu

Corina Secu

Karen Lozano
The University of Texas Rio Grande Valley, karen.lozano@utrgv.edu

Mihail Secu

Mircea Chipara
The University of Texas Rio Grande Valley, mircea.chipara@utrgv.edu

Recommended Citation

Chipara, Dorina Magdalena, Corina Secu, Karen Lozano, Mihail Secu, and Mircea Chipara. "Raman investigations on gamma irradiated iPP-VGCNF nanocomposites: The polymer's tale." Surfaces and Interfaces 17 (2019): 100351. https://doi.org/10.1016/j.surfin.2019.100351

Version of Record: https://www.sciencedirect.com/science/article/pii/S2468023019301877
Manuscript_a0769fd41872dfa5ba956243acf17ddc

Raman Investigations on Gamma Irradiated iPP-VGCNF nanocomposites: The Polymer's Tale

Dorina Magdalena Chipara[1], Corina Secu[2], Karen Lozano[3], Mihail Secu[2], Mircea Chipara[1]

[1]Department of Physics and Astronomy, The University of Texas Rio Grande Valley, 1201 W. University Drive, Edinburg, TX 78539, USA

[2]National Institute for Materials Physics, Magurele, Bucharest, Romania

[2]Department of Mechanical Engineering, The University of Texas Rio Grande Valley, 1201 W. University Drive, Edinburg, TX 78539, USA

SHORT TITLE: Raman on Gamma Irradiated iPP-VGCNF

Corresponding author: Dorina Magdalena Chipara, Department of Physics and Astronomy, The University of Texas Rio Grande Valley, 1201 W. University Drive, Edinburg, TX 78539, USA, e-mail: dorina.chipara@utrgv.edu; Cell 956.607.4950

ABSTRACT

Raman investigations on nanocomposites obtained by loading various amounts of vapor grown carbon nanofibers within an isotactic polypropylene matrix, and gamma irradiated in air, at various integral doses ranging between 0 and 27 kGy, are reported. The analysis is focused on the polymer's answers as revealed by Raman spectroscopy and investigate in detail the effect of ionizing radiation on the position of the Raman line originating from the polymer. The as-obtained data are correlated to the elastic features of the nanocomposites. A competition between gamma irradiation and loading by carbon nanofiber, resulting in the stretching of the polymeric matrix and revealed as a displacement of Raman lines towards smaller wavenumber is reported. It is concluded that side groups (CH_3) are less affected by the loading with carbon nanofibers,

KEYWORDS: Raman; Isotactic polypropylene; Vapor-Grown Carbon Nanofiber; gamma irradiation; molecular elasticity; displacement of the line position

INTRODUCTION

Recent developments in FTIR and Raman spectroscopy allowed for a direct connection between the displacements of the FTIR and/or Raman lines associated to various atomic and molecular vibrations and the local elastic features of matter [1], [2], [3], [4], [5]. The molecular elasticity of polymeric materials is still an incompletely understood topic, to which Raman spectroscopy is now ready to add new details. A quasilinear dependence between the displacement of the position of the Raman lines and the local strain or stress exerted on the sample, was confirmed in the elastic state of the sample for the 2D, G and G' lines of the filler [6], [7], [8], [9].

Typically, Raman spectroscopy may differentiate between atomic and molecular motions occurring in the crystalline and respectively amorphous domains of the polymer; this feature was exploited to estimate the degree of crystallinity in polymers by using Raman spectroscopy [10], [11]. Raman investigations on uniaxial mechanical solicitations in polymers revealed that the applied strain/stress is typically responsible for the displacement of the position of the Raman line towards lower wavenumbers [1], [2], [3], [6], [12], [7], [8], [13]. Compressive forces are responsible for the opposite shift (an increase of the Raman line position as the compressive stress is increased). Due to the mass conservation, the stretching of the polymer generates a compression along the perpendicular direction (Poisson ratio). This implies a potential competition between the tensile and compression distortions for the same chemical bond. Some Raman lines are not essentially affected by the mechanical solicitations; they are associated with chain ends, side chains, or other elastically ineffective bonds.

As a general conclusion, the displacement of the Raman lines due to mechanical strain/stress appears to be linear in the elastic region (where the Hooke's law is valid), generating a linear mapping line position versus strain or stress.

While the displacements of the Raman line positions due to mechanical strain/stress may be quantified, the method is still in its infancy as there is not yet available a detailed and accurate conversion of the measured displacement into strain or stress.

For polymer-based nanocomposites, Raman spectroscopy becomes even more important, as in this case there is no need for an additional external mechanical solicitation. The loading of the polymer with the filler is stretching the macromolecular chains, generated the required strain/stress and finally shifting the position of the Raman line. For such applications, the loading with the nanofiller takes the place of the strain or stress.

The effect of gamma irradiation on the Raman spectra of isotactic polypropylene -vapor grew carbon nanofibers (PP-VGCNFs) nanocomposites is reported and correlated to the atomic and molecular motions occurring within the samples, with emphasize on the polymeric phase.

EXPERIMENTAL METHODS

The iPP-VGCNF nanocomposites were prepared by high shear mixing of isotactic polypropylene (Marlex HLN-120-01) with vapor grown carbon nanofibers (PR-24AG; Pyrograf Products, Inc) by using a HAAKE Rheomix (at 65 rpm and 180 ^{o}C for 9 min followed by an additional mixing at the same temperature and at 90 rpm for 5 min) [14]. Raman measurements have been performed using a Bruker Senterra dispersive Raman microscope spectrometer equipped with a 785 nm laser diode. The resolution of the Raman system was about 1 cm^{-1}. The samples were subjected to ^{60}Co irradiation, at a dose rate of about 1 KGy/h, in air, at room temperature. The final integral doses were 0, 9, 18, and 27 kGy.

EXPERIMENTAL RESULTS

The Raman spectra of iPP-VGCNF nanocomposites irradiated up to different integral doses ranging from 0 to 27 kGy and loaded by various weight concentrations of VGCNFs are shown in Fig. 1.

PLACE OF FIGURE. 1

PLACE OF TABLE 1

Table 1 lists the positions and main parameters of all Raman lines recorded during this study. As a general behavior, it is noticed that the nanofiller decays the amplitude of the Raman lines originating from the polymeric matrix; at concentrations over 10 % wt. VGCNFs, the Raman spectra of the nanocomposites are dominated by the nanofiller's contribution.

Low wavenumber region (below 750 cm^{-1}). The Raman spectra in the low wavenumber region are collected in Fig. 2.

PLACE OF FIGURE 2

Raman lines were observed at 135, 180, 255, 325, 400, 455, 530, and 650 cm^{-1}. The assignments for these lines are included in Table. 1. It is noticed that the increase in the concentration of nanofiller broadens these lines and decreases their amplitude.

PLACE OF FIGURE 3

The most intense line observed within this spectral range is located at 400 cm^{-1} and assigned to the polymeric matrix (CH_2 wagging and CH vibrations) [15], [16], [17]. As noticed from the left panel of Fig. 3, the position of this line (for the pristine polymer) is displaced towards smaller wavenumbers as the integral dose is increased. The shift is consistent with a tensile uniaxial solicitation of the nanocomposite (on the integral dose). The right panel of Fig. 3 shows that the loading with nanofiller strains the macromolecular chain (at 0 kGy) and indicates a competition between dose and loading with VGCNFs. The largest displacement of this line was noticed for the sample loaded by 10 % VGCNF. This line disappears for nanocomposites containing a higher concentration of nanofiller.

Medium wavenumber region (between 750 and 1300 cm^{-1}). The Raman spectra in this wavenumber region are collected in Fig. 4.

PLACE OF FIGURE 4

The main Raman lines noticed within this spectral range were located at 805, 835, 940, 970, 995, 1040, 1100, 1150, 1165, and 1200 cm^{-1}. The assignments of these lines are included in Table 1. The Raman lines of the polymeric matrix are broadened as the loading with VGCNF is increased. The ratio between the intensity of the Raman lines of the polymeric matrix and the main Raman line of the nanofiller (D band) decreases as the loading by VGCNF is increased.

The evolution of the Raman line pair located at 805 and 835 cm^{-1} is of particular interest,

as the line located at about 805 cm^{-1} is typically associated to the crystalline domains of the polymer while the line located at 835 cm^{-1} originates from the amorphous domains [17], [3],[12].

PLACE OF FIGURE 5

The top panel of Fig. 5 shows the effect of ionizing radiation for the pristine polymer, supporting the displacement of the position of the Raman line to smaller wavenumber. The left and right panels of Fig. 5 compare the local elasticity within the crystalline and the amorphous phases. Eventually, it is concluded that the shifts in the amorphous phase are slightly larger than the shifts in the crystalline phase (by about 5 %).

PLACE OF FIGURE 6

Fig.6 collects the Raman spectra recorded in the range 950 to 1020 cm^{-1}, being focused on two lines located at 976 and 998 cm^{-1}. Both lines are originating from the crystalline phase [12], with the line located at 976 cm^{-1} assigned to asymmetric C-C vibrations and rocking CH_3, while the line at 998 cm^{-1} being assigned to rocking CH_3. Typically, the displacements of the Raman line at 998 cm^{-1} (due to irradiation and loading with nanofiller) are slightly weaker than those noticed for the 976 cm^{-1} line. This may reflect the relatively weaker contributions of CH_3 groups, which are not expected to play a direct role in the elasticity of the polymeric matrix but may be significantly affected by crowding (related to the nanofiller).

PLACE OF FIGURE 7

Fig. 7 collects the Raman spectra in the range 2500 to 3100 cm^{-1}, where the maximum wavenumber for the spectrometer used in this research was about 3300 cm^{-1}. Raman spectra (weak and relatively broad) were noticed at 2720, 2840, 2880, and 2960 cm^{-1}. Details about their assignments are included in Table 1. The lines are decaying very rapidly upon loading the polymeric matrix by VGCNFs.

PLACE OF FIGURE 8

Fig. 8 (left panel) shows the Raman spectra for the pristine polymer, subjected to various integral doses at about 2955 cm^{-1}, assigned to asymmetric CH_3 stretching. A weak shift of the Raman line position is noticed. However, this is the smallest shift discussed and reinforces the assumption that CH_3 groups are not strongly involved in the elastic features of the composite. The right panel showed the actual displacement of this line as a function of the integral dose. The line is very sensitive to the loading with VGCNFs and become invisible for loading over 2.5 %.

CONCLUSIONS

Raman investigations on the effect of ionizing radiation (gamma) on iPP-VGCNF nanocomposites, loaded by various amounts of VGCNF are reported.
The Raman line associated with the polymeric matrix are broadened and weaker as the concentration of VGCNF is increased. Technically at (and above) 10 % wt.VGCNFs, the Raman lines are fully washed out by the nanofiller.
The Raman lines originating from the polymeric matrix (pristine) are displaced towards a smaller wavenumber, indicating that the strain of the polymeric matrix is enhanced by irradiation.
Similar results were obtained for the Raman spectra of the polymer filled with nanofibers. A competition between the stretching of the polymeric matrix due to irradiation and to loading with carbon nanofibers was noticed. The Raman line noticed at 400 cm^{-1} was assigned to helical structures in crystalline domains [18].

The pair of Raman lines located at 805 and 835 cm^{-1} was investigated in detail, as the first line originates from crystalline domains and the second one originates from amorphous domains. A slightly larger strain may be noticed in the amorphous domains, based on the Raman displacement.

The pair of Raman lines located at 976 and 998 cm^{-1}, revealed a similar behavior. This was expected as both lines are originating from crystalline domains. The displacement of the line located at 2955 cm^{-1} was significantly weaker than the displacement of the previously mentioned Raman lines. This was expected as this line is connected to CH_3 units-less affected by the loading with nanofiber. It is expected that the observed shifts (of the line a 2955 cm^{-1}) are associated with crowding effects, due to the increase of the concentration of VGCNF.

ACKNOWLEDGMENTS

Authors acknowledge the Department of Defense Grant ‘‘Raman Spectrometer for the Characterization of Advanced Materials and Nanomaterials,’’ W911NF-15-1-0063, the NSF DMR-1523577: UTRGV-UMN Partnership for Fostering Innovation by Bridging Excellence in Research and Student Success and the support of IRASM Centre of Irradiation Technology, “Horia Hulubei” National Institute for Physics and Nuclear Engineering (NIPNE), where the samples irradiation has been performed.

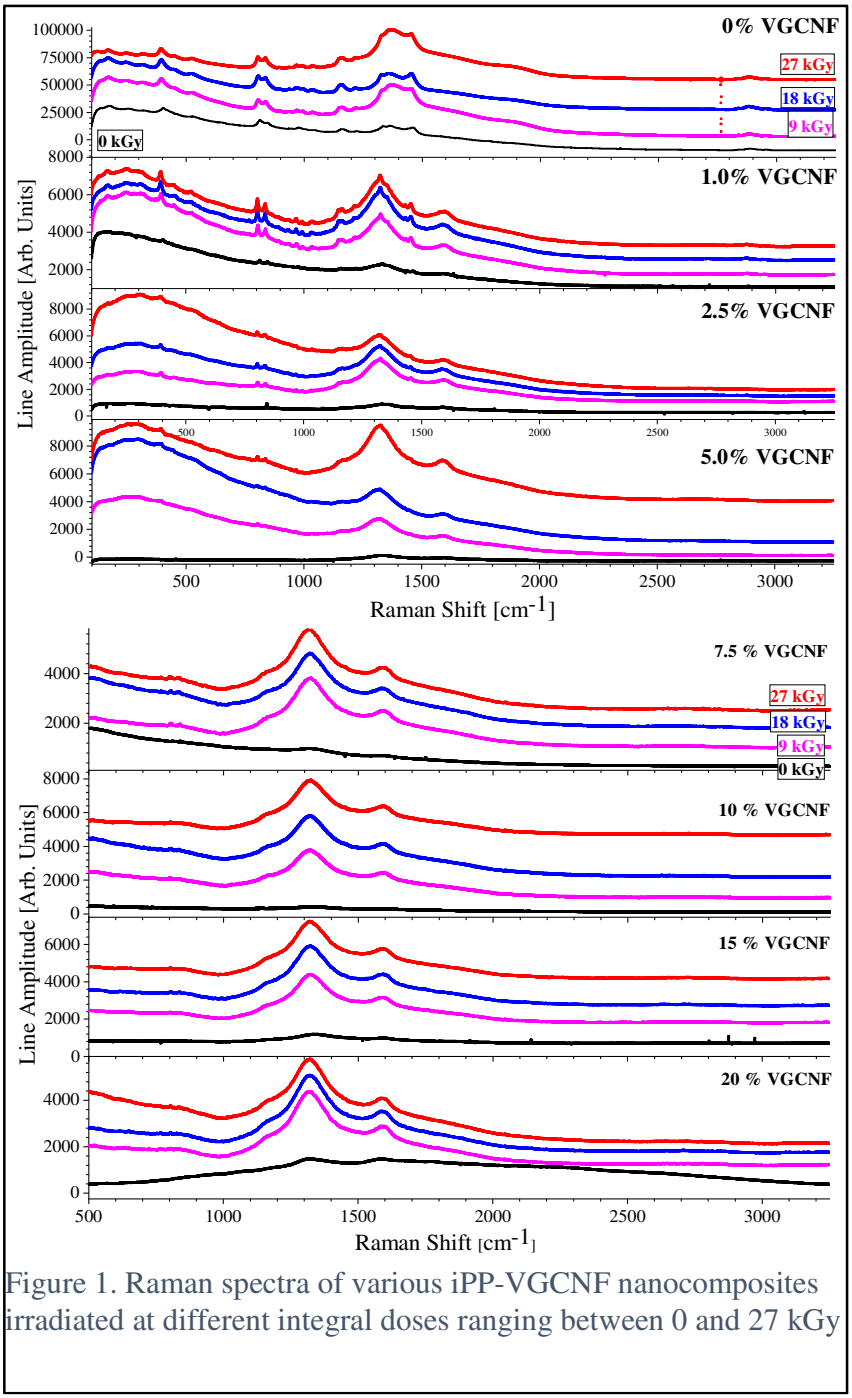

Figure 1. Raman spectra of various iPP-VGCNF nanocomposites irradiated at different integral doses ranging between 0 and 27 kGy

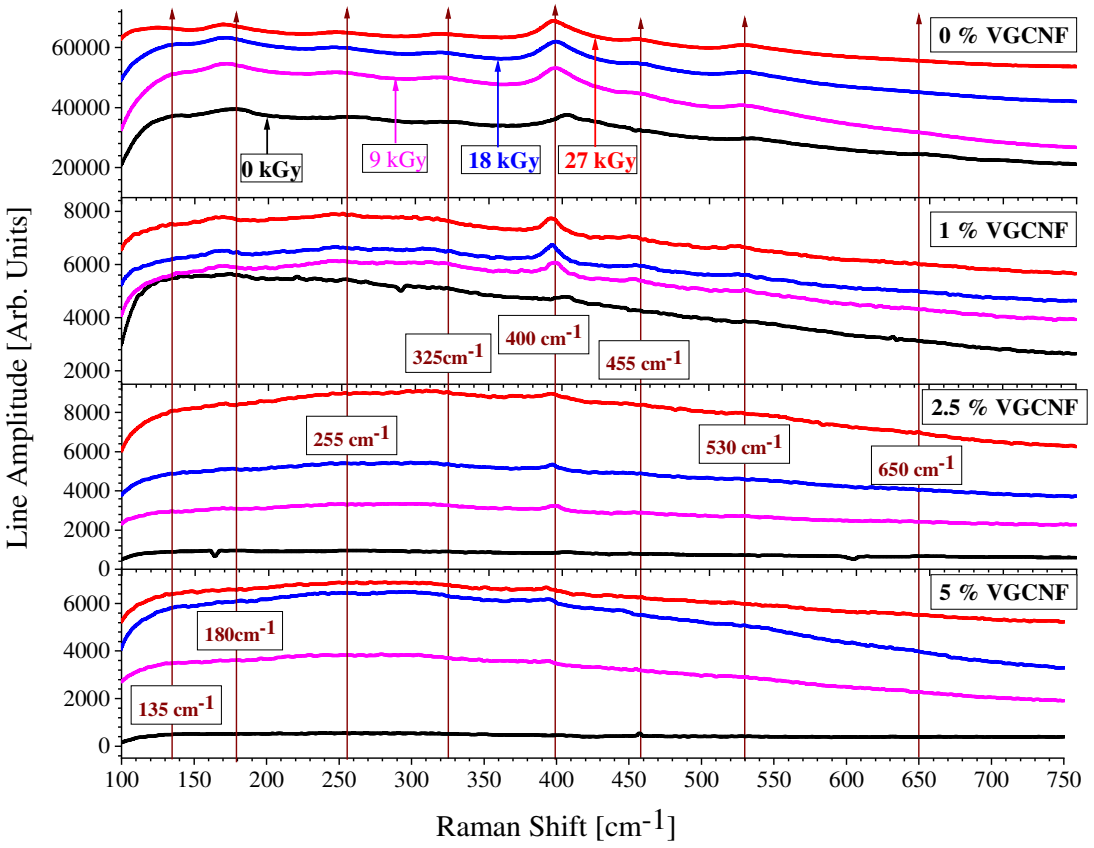

Figure 2. Low wavenumber region of the Raman spectrum for iPP-VGCNF loaded by up to 5.0 % wt. VGCNF, subjected to various integral doses.

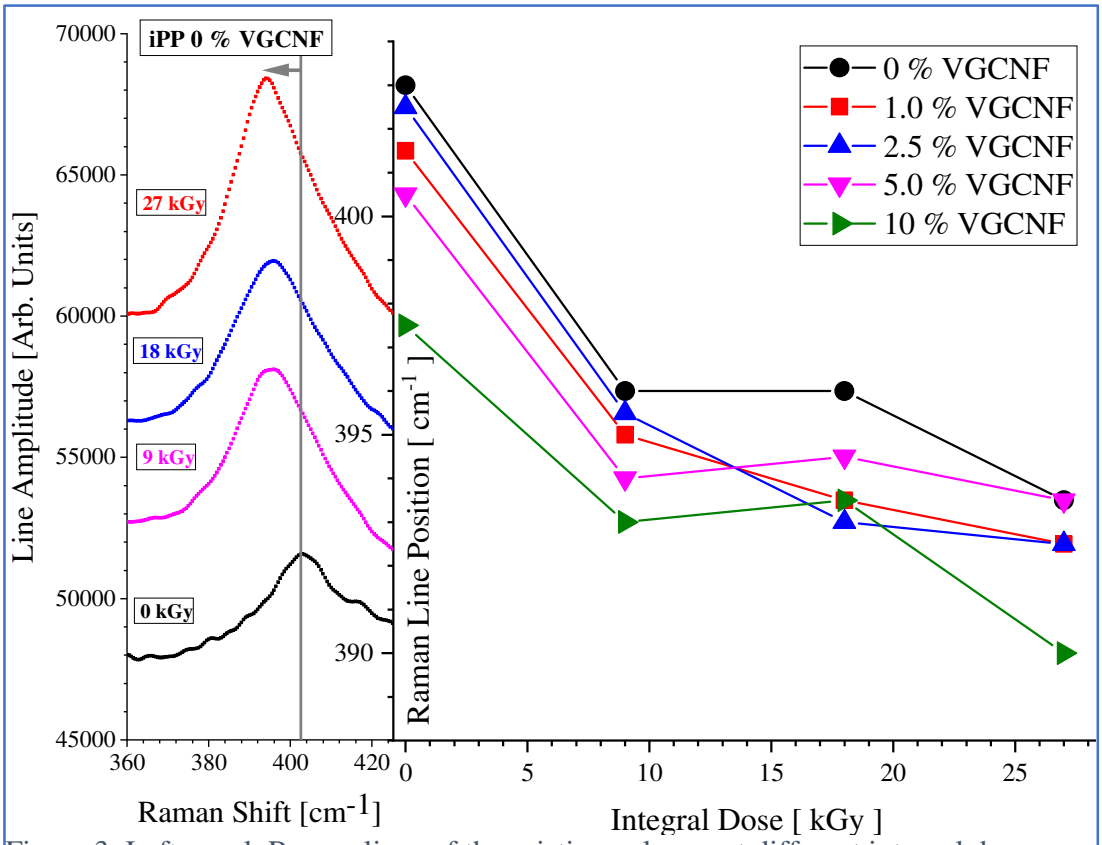

Figure 3. Left panel. Raman lines of the pristine polymer at different integral doses showing the shift of the line located at 400 cm^{-1}. Right panel. The dependence of the resonance line position on the integral dose for iPP-VGCNFs.

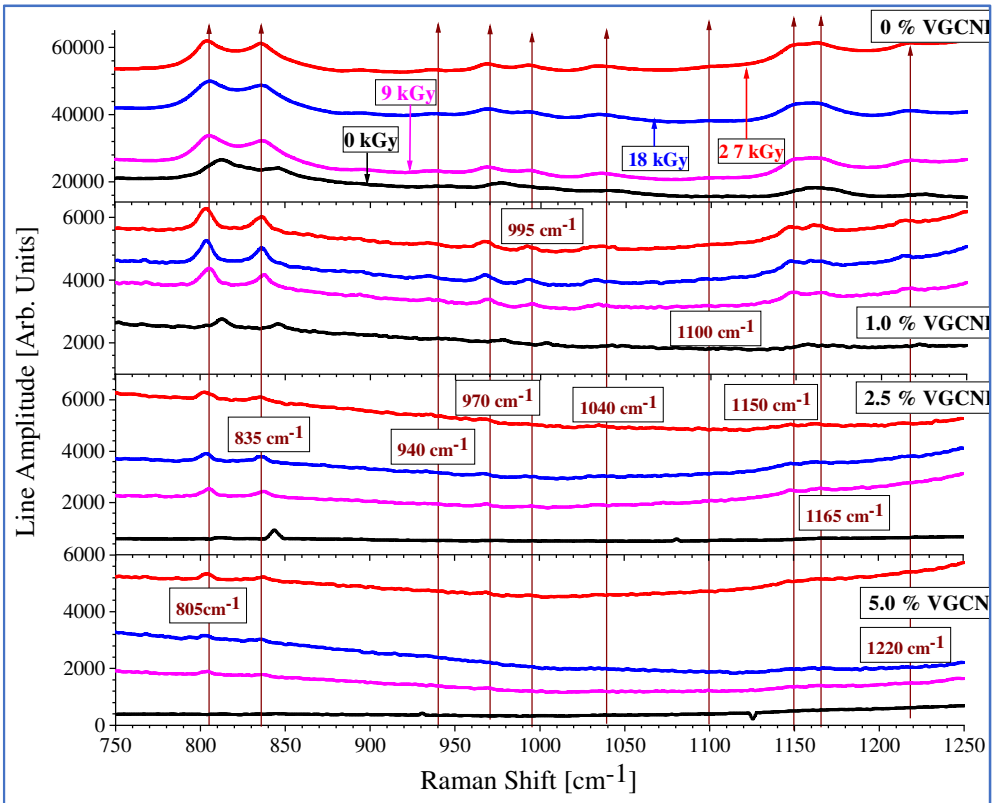

Figure 4 Medium wavenumber region of the Raman spectrum for iPP-VGCNF loaded by up to 5.0 % wt. VGCNF, subjected to various integral doses.

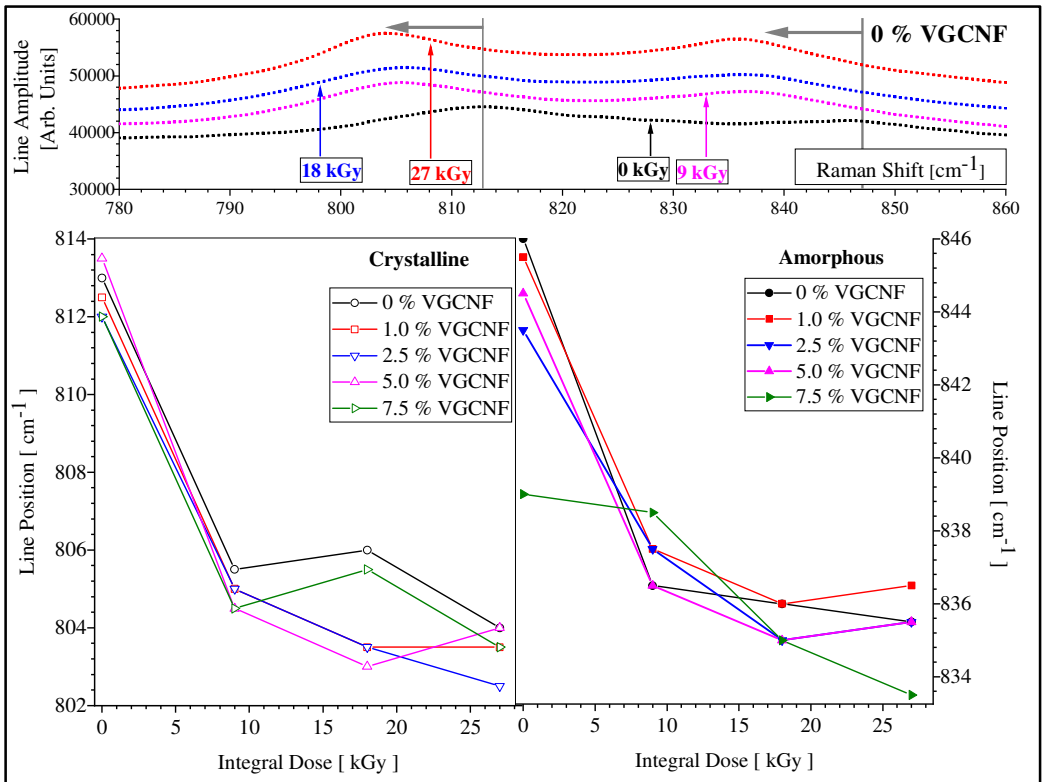

Figure 5. Top panel: Raman spectra of irradiated iPP. Left panel: The dependence of the position of the line located at about 805 cm^{-1} on the integral dose. Right panel: The dependence of the position of the line located at about 835 cm^{-1} on the integral dose.

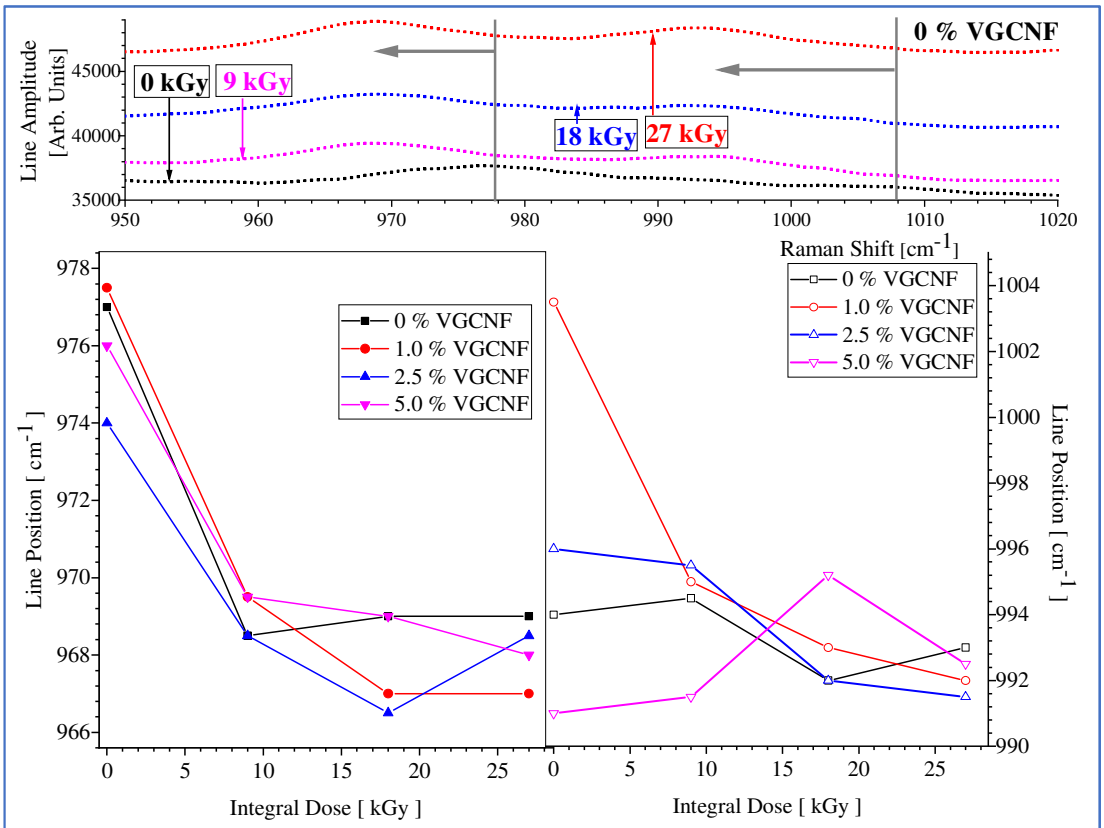

Figure 6. Top panel: Raman spectra of irradiated iPP. Left panel: The dependence of the position of the line located at about 970 cm^{-1} on the integral dose. Right panel: The dependence of the position of the line located at about 997 cm^{-1} on the integral dose.

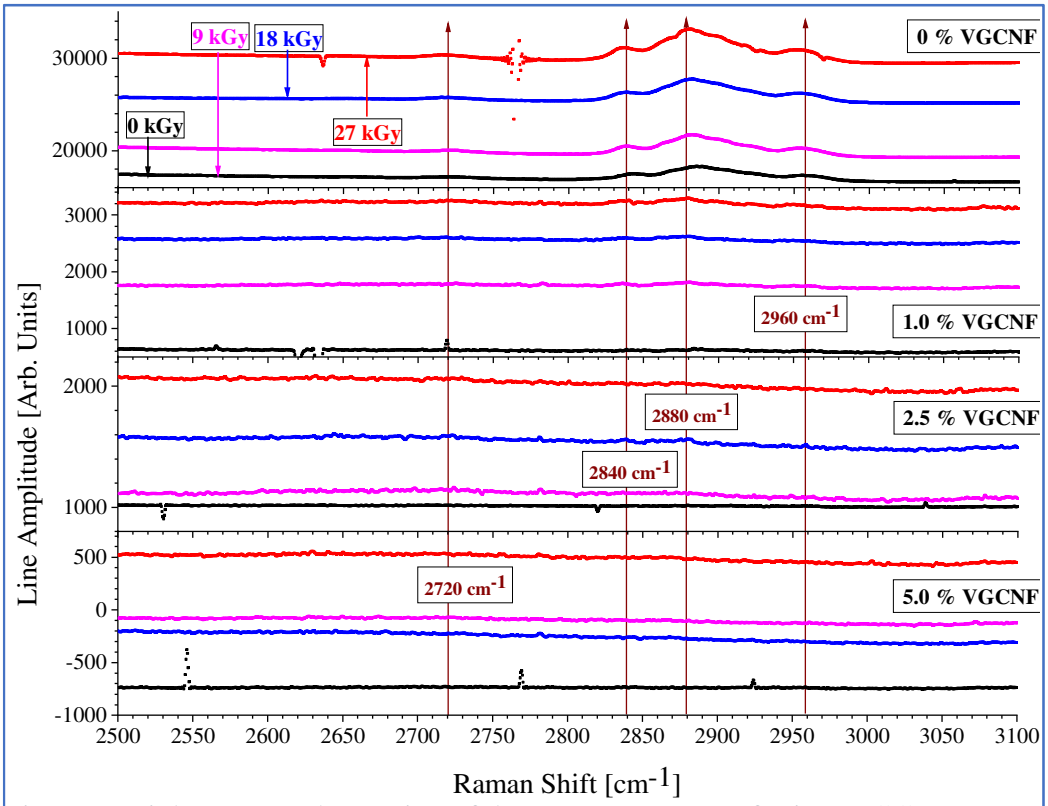

Figure 7. High wavenumber region of the Raman spectrum for iPP-VGCNF loaded by up to 5.0 % wt. VGCNF, subjected to various integral doses.

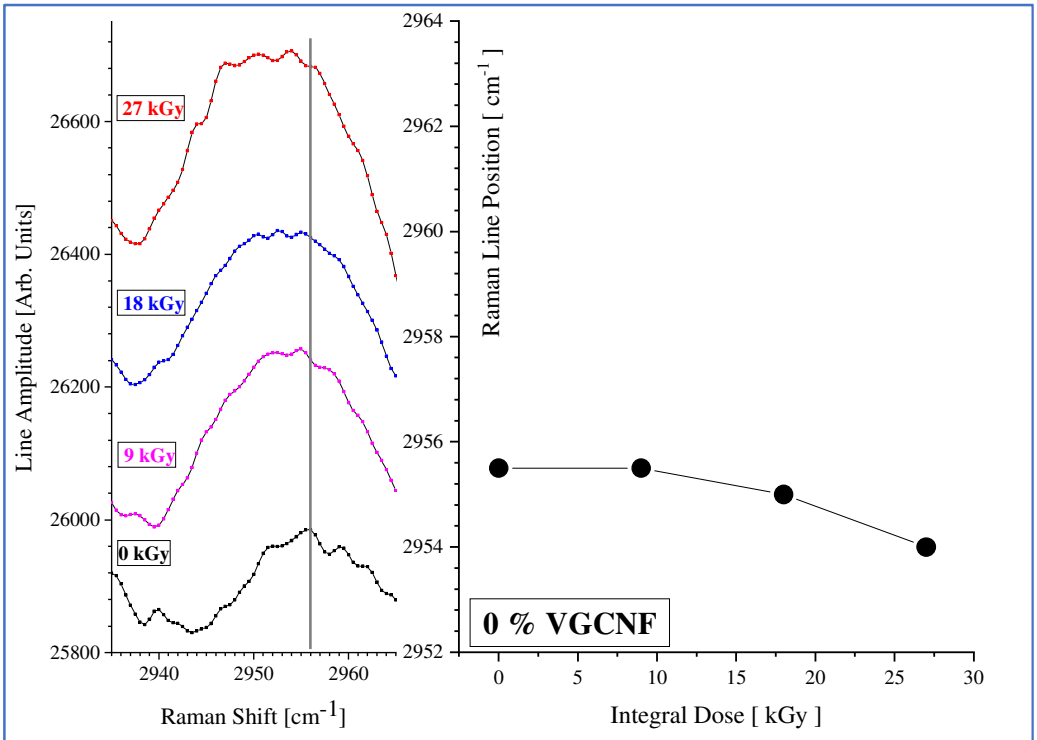

Figure 8. Left panel: Raman spectra of irradiated iPP. Right panel: The dependence of the position of the line located at about 2955 cm^{-1} on the integral dose for the pristine sample.

Table 1.

List of all observed Raman lines for iPP-VGCNF nanocomposites

(for both the polymeric matrix and the nanofiller)

	Observed Position [cm^{-1}]	Reported Position [cm^{-1}]	Assignment	Source	Comments	Ref
1	135			Polymer		[17]
2	180			Polymer		[17]
3	255	252	wCH_2+dCH	Polymer		[17]
3	255	252	wCH_2+dCH			[19]
4	325	321	wCH_2	Polymer		[17]
5	400	398	wCH_2+dCH	Polymer		[17]
6	450	458	wCH_2	Polymer		[17]
7	530	530	wCH_2+vC-CH_3+rCH_2	Polymer		[17]
8	**650**			Polymer		[17]
9	815	809	vCH_2+vC-C+vC-CH	Polymer		[17]
10	815	809	rCH_2+v(C-C)	Polymer	Skeletal, C	[20]
	815	809		Polymer	C	[3]
		830	v(C-C)	Polymer	A	[3]
11	845	841	rCH_2+vC-CH_3	Polymer		[17]
	845	840	rCH_2	Polymer	A+C	[3]
12	895	900	vCH_3+rCH_2+dCH	Polymer		[17]
13	940	940	rCH_2+vC-C (chain)	Polymer		[17]
	940	941		Polymer	Skeletal	[19]
14	978	973	rCH_3+vC-C (chain)	Polymer		[17]
	978	975		Polymer	C	[17]
15	995	998	rCH_3+ wCH_2+dCH	Polymer		[17]
	1040	1034	vC-CH_3+vC-C+dCH	Polymer		[3]
	1160	1152	vC-C+vC-CH_3+dCH+rCH_3	Polymer		[17]
	1160	1152		Polymer	Skeletal	[19]
	1160	1167		Polymer	Skeletal	[19]
	1220	1220	tCH_2+vC-C+dCH	Polymer		[17]
	1220	1219		Polymer	Skeletal	[19]
	1250	1257	dCH+tCH_2+rCH_3	Polymer		[17]
	1335	1330	dCH+tCH_2	Polymer		[17]
	1365	1360	CH_3 symmetric bending+SCH	Polymer		[17]
	1365	1371		Polymer	Skeletal	[19]
	1440	1435	dCH_3 asymmetric	Polymer		[17]
	1465	1457	dCH_3 asymmetric+dCH_2	Polymer		
	2720			Polymer		
	2840	2840	vCH_2	Polymer		

	2880	2883	vCH_3 symmetric	Polymer		
	missing	2920	vCH_2 asymmetric	Polymer		
	2960		vCH_3 asymmetric	Polymer		
		2952	vCH_3 asymmetric			[19]

Abbreviations: v= stretching; d = bending; r=rocking; t=twisting; a=amorphous; c =crystalline; s=amorphous-crystalline

References

[1] S.R. Ahmad, C. Xue, R.J. Young, The mechanisms of reinforcement of polypropylene by graphene nanoplatelets, Mater. Sci. Eng. B Solid-State Mater. Adv. Technol. 216 (2017) 2–9. doi:10.1016/j.mseb.2016.10.003.

[2] T.E. Chang, L.R. Jensen, A. Kisliuk, R.B. Pipes, R. Pyrz, A.P. Sokolov, Microscopic mechanism of reinforcement in single-wall carbon nanotube/polypropylene nanocomposite, Polymer (Guildf). 46 (2005) 439–444. doi:10.1016/j.polymer.2004.11.030.

[3] T. Kida, Y. Hiejima, K.H. Nitta, Molecular orientation behavior of isotactic polypropylene under uniaxial stretching by rheo-Raman spectroscopy, Express Polym. Lett. 10 (2016) 701–709. doi:10.3144/expresspolymlett.2016.63.

[4] M. Chipara, J. Hamilton, A.C.A.C. Chipara, T. George, D.M.D.M. Chipara, E.E.E.E. Ibrahim, K. Lozano, D.J.D.J. Sellmyer, Fourier Transform Infrared Spectroscopy and Wide-Angle X-ray Scattering : Investigations on Polypropylene – Vapor- Grown Carbon Nanofiber Composites, J. Appl. Polym. Sci. 125 (2012) 353–360. doi:10.1002/app.

[5] M. Chipara, J.R. Villarreal, M.D. Chipara, K. Lozano, A.C. Chipara, D.J. Sellmyer, Spectroscopic investigations on polypropylene-carbon nanofiber composites. I. Raman and electron spin resonance spectroscopy, J. Polym. Sci. Part B Polym. Phys. 47 (2009) 1644–1652. doi:10.1002/polb.21766.

[6] T.M.G. Mohiuddin, A. Lombardo, R.R. Nair, A. Bonetti, G. Savini, R. Jalil, N. Bonini, D.M. Basko, C. Galiotis, N. Marzari, K.S. Novoselov, A.K. Geim, A.C. Ferrari, Uniaxial strain in graphene by Raman spectroscopy: G peak splitting, Grüneisen parameters, and sample orientation, Phys. Rev. B - Condens. Matter Mater. Phys. 79 (2009). doi:10.1103/PhysRevB.79.205433.

[7] H.D. Wagner, M.S. Amer, L.S. Schadler, Residual compression stress profile in high-modulus carbon fiber embedded in isotactic polypropylene by micro-Raman spectroscopy,

Appl. Compos. Mater. 7 (2000) 209–217. doi:10.1023/A:1008956929081.

[8] Z. Liu, J. Zhang, B. Gao, Raman spectroscopy of strained single-walled carbon nanotubes, Chem. Commun. (2009) 6902–6918. doi:10.1039/b914588e.

[9] C.C. Chang, C.C. Chen, W.H. Hung, I.K. Hsu, M.A. Pimenta, S.B. Cronin, Strain-induced D band observed in carbon nanotubes, Nano Res. 5 (2012) 854–862. doi:10.1007/s12274-012-0269-3.

[10] L. Valentini, J. Biagiotti, M.A.A. López-Manchado, S. Santucci, J.M.M. Kenny, Effects of Carbon Nanotubes on the Crystallization Behavior of Polypropylene, Polym. Eng. Sci. 44 (2004) 303–311. doi:10.1002/pen.20028.

[11] A.S. Nielsen, D.N. Batchelder, R. Pyrz, Estimation of crystallinity of isotactic polypropylene using Raman spectroscopy, Polymer (Guildf). 43 (2002) 2671–2676.

[12] J. Martin, M. Ponçot, J.M. Hiver, P. Bourson, A. Dahoun, Real-time Raman spectroscopy measurements to study the uniaxial tension of isotactic polypropylene: A global overview of microstructural deformation mechanisms, J. Raman Spectrosc. 44 (2013) 776–784. doi:10.1002/jrs.4244.

[13] M. Mu, S. Osswald, Y. Gogotsi, K.I. Winey, An in situ Raman spectroscopy study of stress transfer between carbon nanotubes and polymer, Nanotechnology. 20 (2009). doi:10.1088/0957-4484/20/33/335703.

[14] M. D. Chipara, K. Lozano, A. Hernandez, M. Chipara, TGA analysis of polypropylene-carbon nanofibers composites, Polym. Degrad. Stab. 93 (2008) 871–876. doi:10.1016/j.polymdegradstab.2008.01.001.

[15] M. Tobin, THE INFRARED SPECTRA OF POLYMERS. III. THE INFRARED AND RAMAN SPECTRA OF ISOTACTIC POLYPROPYLENE, J. Phys. Chem. 64 (1960) 216–219. http://pubs.acs.org/doi/abs/10.1021/j100831a007 (accessed June 14, 2012).

[16] T. Sundell, H. Fagerholm, H. Crozier, Isotacticity determination of polypropylene using FT-Raman spectroscopy, Polymer (Guildf). 37 (1996) 3227–3231.

[17] M. Arruebarrena de Baez, M. Hendra, P.J.; Judkins, The Raman Spectra of Oriented Isotactic Polypropylene, Spectrochim. Acta. A. Mol. Biomol. Spectrosc. 51 (1995) 2117–2124.

[18] M.S. Sevegney, R.M. Kannan, A.R. Siedle, R. Naik, V.M. Naik, Vibrational spectroscopic investigation of stereoregularity effects on syndiotactic polypropylene structure and morphology, Vib. Spectrosc. 40 (2006) 246–256. doi:10.1016/j.vibspec.2005.10.003.

[19] J.F. Gillespie, J.W.L. Fordham, Infrared and Raman Spectoscopy of Popypropylene, in: Ind. Eng. Chem., 1959: pp. 1365–1368. doi:10.1021/ie50599a030.

[20] K.G. Gatos, C. Minogianni, C. Galiotis, Quantifying Crystalline Fraction within Polymer Spherulites, Macromolecules. 40 (2007) 786–789. doi:10.1021/ma0623284.